Int J Adv Manuf Technol (2017) 91:2077–2088
DOI 10.1007/s00170-016-9728-4

ORIGINAL ARTICLE

Controlling of material flow in the quasi-bulk forming of thin-walled corrugated rings through optimization of contact pressure

Nan Xiang[1] · **Zhong-jin Wang**[1] · **Jun Yi**[1] · **Hui Song**[1]

Received: 9 June 2016 / Accepted: 7 November 2016 / Published online: 30 December 2016
© Springer-Verlag London 2016

Abstract Corrugated rings made of difficult-to-deform superalloy sheet with extremely thin wall are hardly manufactured since the forming processes are rather sensitive to parameters, such as axial feeding, cavity pressure, contact pressure, and so forth. The quasi-bulk forming method proposed in the author's previous work, which gets rid of axial compression, was demonstrated to be an effective solution. In this work, forming strategy based on the controlling of material flow in this process is further developed. Since the pressure-carrying medium (i.e., viscous medium) is of high viscosity, the sealing pressure of this process is lowered down in comparison with that of forming processes utilizing nonviscous fluid as forming medium. The contact pressure at blank ends becomes adjustable as a result. Effects of contact pressure at sealing/blank interface (P_m) on the blank draw-in were investigated numerically. An optimal load path of P_m was obtained. Regulatory mechanism of contact pressure was presented, and contact pressure was considered to be the resultant pressure caused by the static pressure (P_s) and cavity pressure (P_v). Thereafter, process optimization was conducted through adjusting the path of P_v to approximate to the optimal path of P_m. On the basis of that, geometrical parameters of die cavity were improved and forming experiments were conducted accordingly to form two sorts of nickel-based superalloy corrugated rings. Sufficient blank draw-in was observed and thickness thinning is acceptable. The forming strategy, which is based on the adjustment of contact pressure, was verified to be feasible to improve the manufacturability of thin-walled corrugated rings.

Keywords Quasi-bulk forming · Viscous medium · Material flow · Nickel-based superalloy · Contact pressure

By employing viscous medium as forming medium instead of fluid or gas, sealing limit of the quasi-bulk forming process is lowered down.
Forming window of corrugated rings manufacturing process is extended due to the decrease of sealing limit.
The contact pressure at blank ends can be adjusted to adapt to the material flow in the forming process.
Based on this forming strategy, two types of nickel-based superalloy parts were manufactured, which validates the feasibility.

✉ Zhong-jin Wang
wangzj@hit.edu.cn

Nan Xiang
xiangnan-87@163.com

[1] National Key Laboratory for Precision Heat Processing of Metals, Harbin Institute of Technology, Harbin 150001, China

1 Introduction

Thin-walled tubular parts, conventionally made of high strength alloy, are effective to reduce weight of equipment and improve the performance, thus gain widespread industrial application ranging from piping system, vacuum engineering, chemical engineering, and to aerospace manufacturing. Several methods have been used to manufacture thin-walled tubular parts with complex shapes, such as tube hydroforming (THF) process based on the combined action of fluid pressure and axial feeding [1, 2], superplastic forming (SPF) process employing gas pressure together with axial compression [3, 4], tube gas forming technique [5, 6], lateral extrusion of pipes with a lost core (LELC) [7, 8], semi-dieless forming process based on local induction heating and axial compression [9], and water jet incremental forming process [10]. Essentially, all these forming processes were implemented in the condition

that internal support was adopted, and tubes were compressed under axial load at the same time. Based on this strategy, the controllable metal flow of tubular blank into the die cavity is achieved. However, with the increase of the forming difficulties caused by the high complexity of desired components and the high strength of raw material, the stable and homogenous metal flow tends hardly to be accomplished, which consequentially leads to forming drawbacks like buckling, wrinkling, or fractures.

Some researchers concentrate on using control strategies to alter technological parameters to adapt to the deformation behaviors of metal blank. Lorenzo et al. optimized internal pressure path in THF process for Y-shaped tubes by using gradient-based decomposition approach [11]. Forming defects such as underfilling or ductile fractures were avoided properly. Louh et al. studied the influence of bilinear pressure path on corner filling of box-shaped tubes in the hydroforming process and presented an improved pressure path [12]. Faraji et al. investigated process parameters in the forming of CuSn6 metal bellows and indicated that increase in internal pressure leads to bursting and axial feeding of tube material is closely related to thickness thinning as well [13]. Kang et al. studied the bellows hydroforming process with internal pressure without axial feeding and stated that geometrically unstable metal flow caused by the lack of axial feeding is the primary cause of bulge fractures [14]. In order to evaluate the effect of pressure path on the forming of metal bellows, Bakhshi-Jooybari et al. proposed a comprehensive forming window and pointed out that the pressure path influences the occurrence of bursting or wrinkling defects in the products [15]. In summary, internal pressure path and material feeding history are two essential process parameters in THF process.

Yet, for ring-shaped parts with larger outer diameter and extremely thin wall, axial compression cannot be equally imposed on the axial ends of metal blank. In this case, the quasi-bulk forming process without use of axial compression was demonstrated to be beneficial to the fabrication of thin-walled corrugated rings [16, 17]. But, there is a premise that ring-shaped blank is properly fed into die cavity. If axial compressive load is removed, metal flow will be more sensitive to the frictional force at the blank/die interface. That is significantly influenced by the sealing pressure at both ends of the ring-shaped blank. Then, it is inferred that reducing sealing pressure will be advantageous to decrease frictional force and improve metal flow. As a result, technological means by which sealing pressure can be adjusted properly should be developed.

Hein once proposed a process window of blank hydroforming process as shown in Fig. 1. The sealing limit is considered as a threshold of this process window [18]. Obviously, sealing limit is determined by flange contact pressure and cavity pressure. Bringing down the contact pressure may lower down the sealing limit and extend the forming range. Similarly, if this concept is introduced into the field of tube forming, the potential technical means to facilitate the metal flow can be deduced as follows: reducing cavity pressure, diminishing contact pressure at seal ring/blank interface, and selecting forming medium easy to be sealed.

Rosel and Merklein focused on improving the sealing performance in hydroforming by using a kind of unique fluid as forming medium [19]. In their study, magnetorheological (MR) fluid serving under a regionally applied magnetic field acts as sealing medium. Compared with conventional fluid medium in hydroforming, such as mineral oil, the sealing limit was reduced effectively and the thickness thinning was lowered accordingly. It is attributed to the increase of regional MR fluid viscosity under the external magnetic field. The drawback of this technology is the complicated equipment and process control.

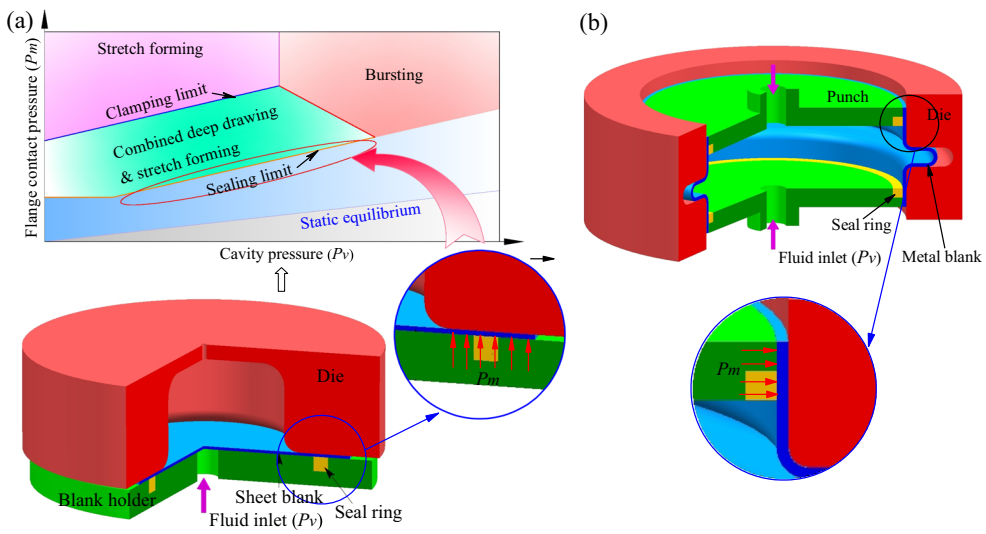

Fig. 1 Process window for blank hydroforming (**a**, according to [18]) and tube forming process with internal pressure without axial feeding (**b**)

However, on the basis of this strategy, forming medium such as viscous medium (i.e., a type of highly viscous polymer employed in previous proposed quasi-bulk forming process) will probably be appropriate to lower down the sealing limit and extend forming window. Viscous medium is semi-solid at room temperature. Meanwhile, viscous medium with different viscosity can be synthesized. With the increase of viscosity, the traits of viscous medium gradually changes from liquid-like state to solid-like state [20]. In comparison with fluid medium, viscous medium is more easily to be sealed. In other words, sealing limit (defined by Eq. 1) is decreased from the indication of Fig. 1a. That is to say, in the condition that cavity pressure keeps constant, contact pressure at blank/die interface may decrease with reducing of sealing limit [19, 21], which will lower down the frictional force at the blank/die interface. Hence, the metal flow into the die cavity will be improved. Due to aforementioned advantages of viscous medium, the material feeding will be adjustable. The application of this method on thin-walled, complex-shaped tubular parts will be expectable.

$$\text{sealing limit} = \frac{P_m}{P_v} \tag{1}$$

where P_m and P_v refer to contact pressure and cavity pressure, respectively.

In this paper, an optimization strategy based on the improvement of material flow in the quasi-bulk forming of thin-walled corrugated rings was studied. By employing a special sealing strategy, the contact pressure between seal ring and metal blank can be adjusted to fit with the forming of desired product. Concretely, several patterns of contact pressure paths were introduced to examine the effects of contact pressure on metal flow numerically. The optimal loading path of contact pressure was obtained from finite element analysis (FEA). Then, the sealing strategy of viscous medium, which aims at facilitating the adjustment of contact pressure, was proposed. In this sealing condition, influences of static pressure on blank draw-in were investigated experimentally. Meanwhile, a new process design based on the optimal loading path of contact pressure was presented. Finally, forming experiments were conducted to verify the feasibility of this design strategy.

2 Experimental condition and research methodology

The ring-shaped blank made of stainless steel SUS321 and nickel-based superalloy GH4169 sheet was used to fabricate thin-walled corrugated rings. GH4169 is a commercial alloy with the same nominal composition with Inconel 718 in US [22]. It possesses good corrosion resistance, higher tensile strength, and excellent welding performance [23, 24]. The uniaxial tensile test of GH4169 sheet was carried out at room temperature and the resulting true stress-strain curve is shown in Fig. 2. Table 1 gives mechanical properties of SUS321 sheet.

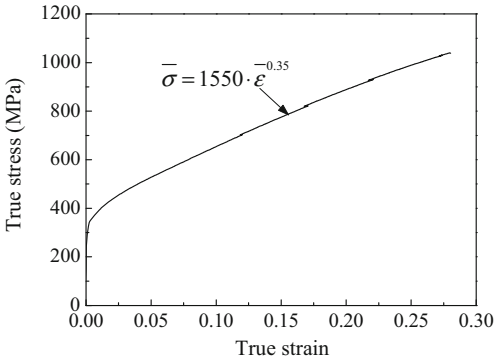

Fig. 2 Constitutive relationship of GH4169 sheet

Table 2 gives mechanical properties of viscous medium. The constitutive relationship of viscous medium is defined as $\overline{\sigma} = c\overline{\varepsilon}^{m}$, where c and m are given in Table 2. The combination of extrusion test and the corresponding FEA was conducted to get the flow stress-strain rate curves of viscous medium. Then, nonlinear fitting method was employed to determine the accurate value of c and m in constitutive equation by getting close to these curves through repeated trials [25]. The die set is clamped by the universal hydraulic press. Viscous medium is injected into deformation regions with the maximum pressure of 250 MPa.

The manufacturing processes and research methodology are illustrated in Fig. 3. Sheet metal strip was used to produce ring-shaped blank through rolling and welding. Then, the ring-shaped blank is positioned in the die set. Viscous medium is injected into the outer side of metal blank. Metal blank is pushed into the die cavity to acquire the form of the die. Thereafter, depressurize and open the die set to get the final product. Effects of contact pressure and cavity pressure on material flow in the forming step were studied through following procedures. Firstly, finite element analysis of the optimal contact pressure path was conducted to examine the effects of contact pressure on metal flow basically. Then, process optimization was presented, which aims at minimizing contact pressure and cavity pressure. Finally, forming experiments were conducted to verify the feasibility of the optimization strategy.

Table 1 Mechanical properties of SUS321 sheet [26]

YS, σ_s (MPa)	UTS, σ_b (MPa)	Elastic modulus, E (GPa)	Strength coefficient, K (MPa)	Hardening exponent, n
206	539	200	980	0.34

Table 2 Mechanical properties of viscous medium

Molecular weight (g/mol)	Viscosity (kPa·s)	Strain rate sensitive exponent, m	Strength coefficient, c	Poisson ratio
500,000	17	0.25	0.24	0.47

3 Finite element analysis

3.1 Finite element model

Commercial finite element code ANSYS/LS-DYNA was used for FEA. Finite element model shown in Fig. 4 was established to study the simple diameter reducing process. 1/4 of circumferential direction and 1/2 of the meridian direction were selected in the modeling due to the axial symmetry. Dimensions of model and friction coefficient at the interface are given in Table 3. Coulomb friction model was adopted when setting the contact condition at all interfaces. Frictional coefficients were given by taking the studies of Liu et al. and Ahmetoglu et al. as references. The ring-shaped blank was modeled with Belytschko element and meshed with quadrilateral, yet longitudinal welding line was not taken into consideration. Viscous medium was meshed with hexahedral element (solid 164). Seal ring was modeled with shell element (Belytschko) and defined by a nonlinear elastic material model (Blatz-Ko). The piston pushed the viscous medium to raise the forming pressure. The contact pressure (P_m) was applied on the normal direction of seal ring surface separately; namely, it is independent of the cavity pressure, which facilitates the investigation of contact pressure.

3.2 Validation of finite element results

In order to confirm the feasibility of the proposed finite element model, finite element results obtained in different stages of the forming process are compared with experimental conditions. Figure 5 gives the comparison of finite element and experimental results. In the initial stage of the diameter-reducing process, wrinkling probably occurs due to the circumferential shrink of the ring-shaped blank (see Fig. 5a).

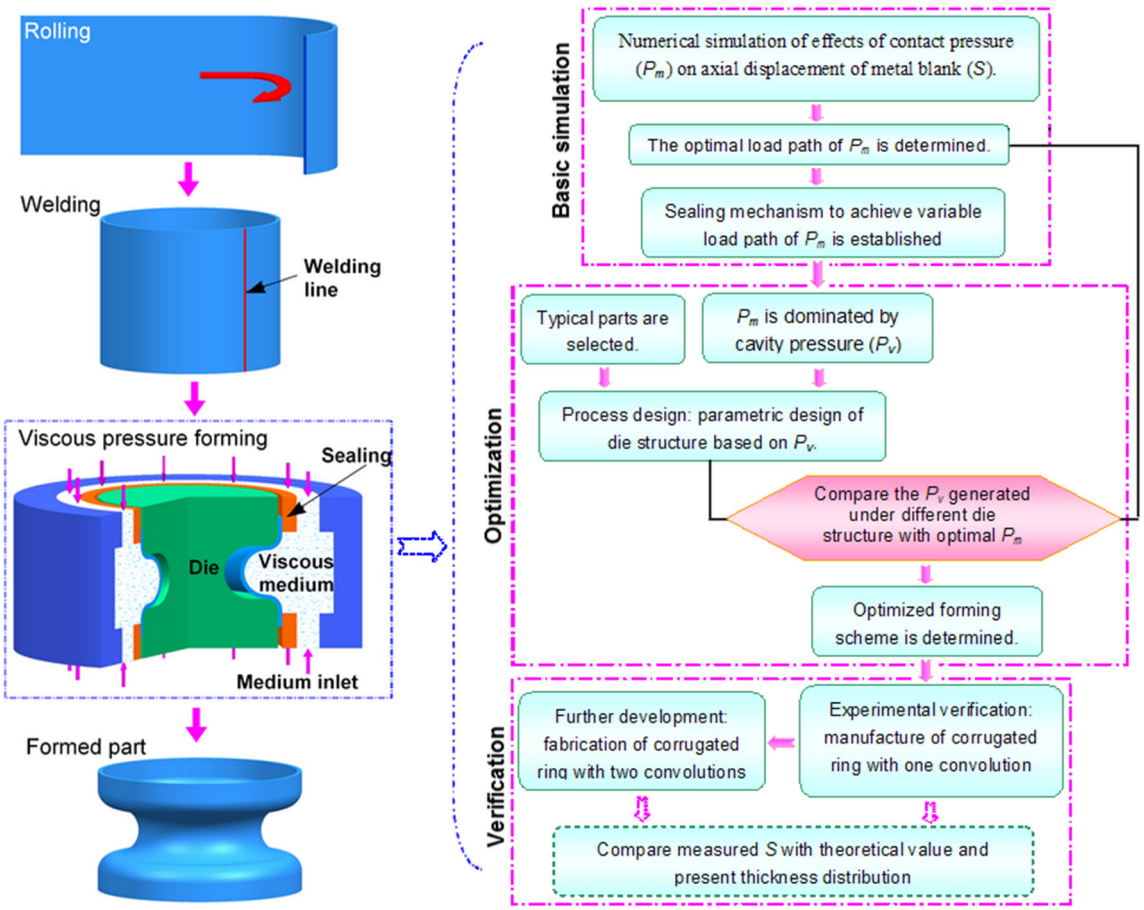

Fig. 3 Mechanism of the process optimization based on the adjustment of contact pressure at blank ends in the manufacture of corrugated rings

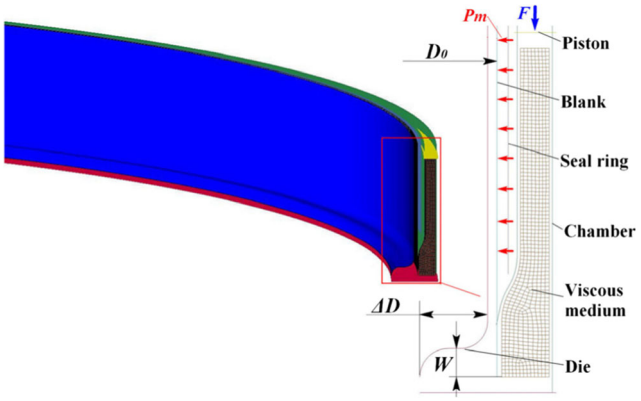

Fig. 4 Finite element model

Through reducing the die radius at the entrance of deformation zone, the wrinkling tendency is eliminated (see Fig. 5b). The occurrence and disappearance of wrinkling is predicted properly. As to forming experiments which aim at producing specific components through diameter-reducing process, fracture may appear at the root of corrugation in the condition that the root radius of female die is too small. Finite element model which is similar to the FE model shown in Fig. 4 was established. The fracture is also predicted by FEA through the formability diagram. In general, by employing finite element model established in this paper, forming defects in diameter reducing process of the ring-shaped blank can be predicted. The finite element model is considered to be feasible for the prediction of metal flow and thickness distribution in this work.

3.3 Effects of contact pressure on end displacement of the ring-shaped blank

Contact pressure between the ring-shaped blank and seal ring determines the frictional force at the seal ring/blank interface. With the increase of contact pressure, blank draw-in decreases and excessive thinning or fracture gradually becomes the main failure mode because of the metal blank is stretched. Suppose contact pressure is applied independently and the load path of contact pressure can be designated theoretically, the influence of contact pressure on metal flow is probably simulated.

Nine theoretical load paths for contact pressure (P_m) were selected to study the influence of contact pressure on axial displacement of the ring-shaped blank (see Fig. 6). Contact pressure (P_m) at seal ring/blank interface is illustrated in Fig. 7a. End displacement of the ring-shaped blank (S) is used to evaluate the axial movement of metal blank. The value of end displacement obtained from FEA is shown in Fig. 7b. The value of S under the action of load path 1 and load path 9 are respectively 1.00 and 0.94, which are remarkably larger than those of other types of contact pressure paths. For load path 1, contact pressure is a constant value of 10 MPa, which is impractical. Load path 7 shows the same variation tendency as load path 9, but the contact pressure in each load point of load path 7 is larger than that in load path 9. Thus, the axial displacement is smaller. The value of S corresponding to load path 8 is 0.75, which shows a 20.2% decrease compared with that under load path 9. For load path 9, the contact pressure reaches 40 MPa (i.e., 50% of the largest contact pressure) when the piston stroke rises to 80% of the total stroke. That is to say, contact pressure in initial stage of the forming process is small and increases to a large value in the final stage. Yet, the load path 8 shows a completely opposite type.

Figure 7c, d presents the ratio of velocity difference between viscous medium and metal blank for two typical load paths of P_m (i.e., load path 8 and load path 9). In each case, three characteristic zones were selected for comparison. Velocity difference for each zone under load path 8 is larger than that under load path 9. The maximum velocity difference at die radius region (zone B) is 23.8 and 13.0% for load path 8 and load path 9, respectively. Since metal blank is pushed into die cavity by viscous medium, the large velocity difference means that metal flow is restricted to some degree. Obviously, load path 9 of P_m facilitates metal flow more than load path 8 does, which coincides with the results of end displacement. Then, it can be inferred that a smaller contact pressure in initial stage results in a smaller resistance for metal flow along meridian direction, thus the material of ring-shaped blank enters into the die cavity more smoothly. As to the final stage of the forming process, though the contact pressure increases sharply, the resistance along meridian direction will not increase distinctly since the axial displacement in initial stage reduces the contact area between the ring-shaped blank and seal rings. On the contrary, the axial displacement of the ring-shaped

Table 3 Parameters in FEA

Initial tube diameter, D_0 (mm)		230
Initial wall thickness of ring-shaped blank, t_0 (mm)		0.3
Longitudinal width of corrugation, 2 W (mm)		1.4
Half of diameter reduction after forming, $\Delta D/2$ (mm)		4.0
Coulomb friction coefficient	Tube/viscous medium interface, μ	0.20 [25]
	Tube/die interface, μ_s	0.05 [25, 27]

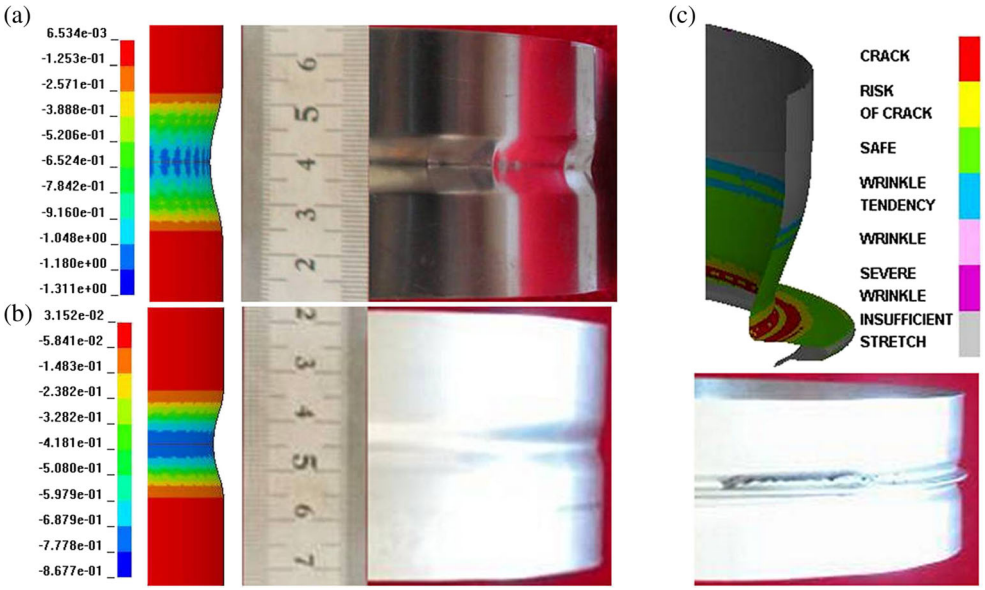

Fig. 5 Prediction of forming defects by FEA in diameter reducing process. **a** Thickness thinning ratio and acceptable workpiece (initial stage). **b** Thickness thinning ratio and wrinkled workpiece (initial stage). **c** Formability diagram and fractured workpiece

blank is restrained severely like the condition under load path 8. In general, S can be adjusted by employing different contact pressure path, and contact pressure path 9 is considered to be the optimal one among all load paths.

4 Results and discussion

4.1 Establishment of sealing mechanism

In order to make the contact pressure adjustable in practical production, a special sealing structure for viscous medium was proposed as illustrated in Fig. 8. Type "YX" seal rings made of polyurethane are positioned in the groove of container. The outside and inside surface of seal rings contact with the ring-shaped blank and container, respectively. A cover plate is placed on the top of seal rings and fixed with dies. Thus, seal rings deform under static compressive load caused by the cover plate, which is recognized as (P_s). With the increase of cavity pressure (P_v), seal ring is forced to contact with tubular blank and container firmly. Then, the leakage of viscous medium is avoided. Seal rings are compressed under the combined action of P_s and P_v, and the elastic deformation of seal rings results in the total contact pressure (P_m) at seal ring/blank interface.

Static pressure (P_s) is related to the dimensions of seal rings and can be modified through selecting seal rings with different initial height (H_0, see Fig. 8a) and width (L_0). Effects of P_s on metal flow were measured experimentally. The ring-shaped blank with initial diameter of 230 mm and initial wall thickness of 0.3 mm, which is made of SUS321 sheet, was employed. The axial displacement (S) of the ring-shaped blank corresponding to different types of seal rings is presented in Table 4. S corresponding to "type 1" and "type 9" seal rings are respectively 0.92 and 1.05 mm, which shows a 14% increase. That is to say, metal flow towards the die cavity is improved. It is resulted from the fact that seal rings are compressed more severely with the increase of H_0 and L_0; thus, the

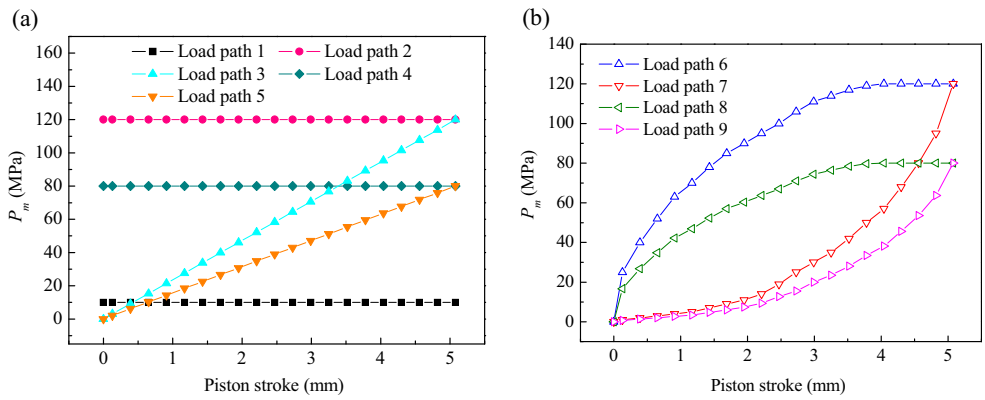

Fig. 6 Nine types of contact pressure paths acting on metal blank. **a** Linear type. **b** Nonlinear type

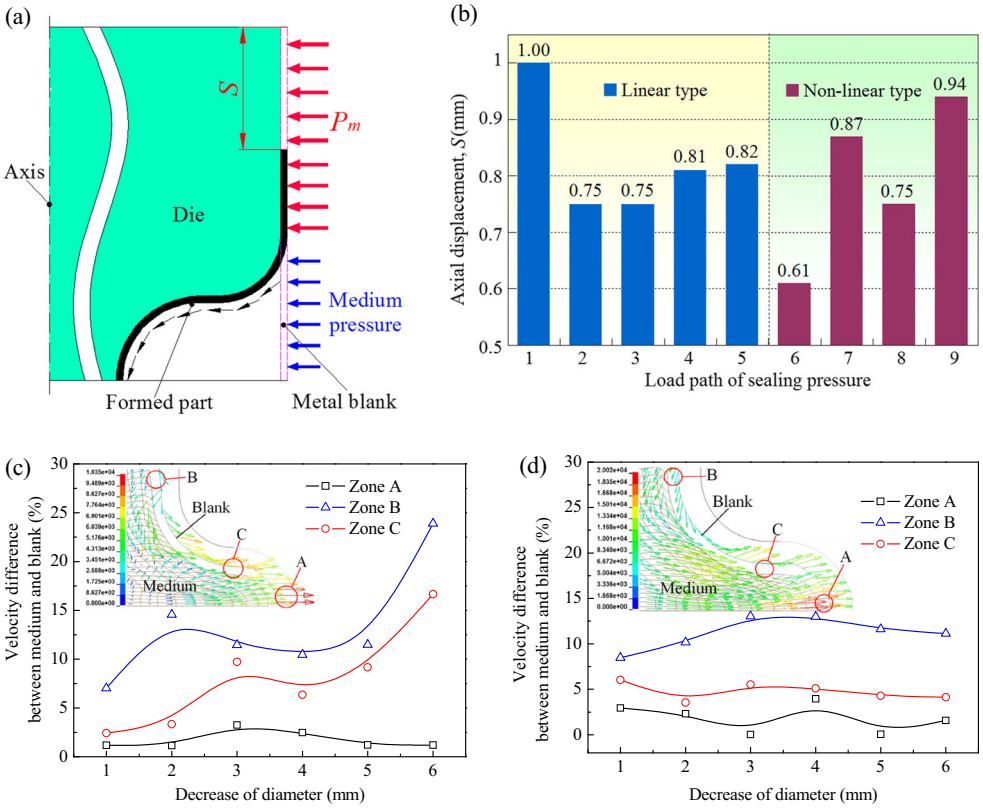

Fig. 7 End displacement and velocity difference between medium and blank corresponding to different load path of P_m. **a** Illustration of P_m. **b** Axial displacement of ring-shaped blank (S). **c** Velocity difference for load path 8. **d** Velocity difference for load path 9

frictional resistance at the ends of the ring-shaped blank increases accordingly. Therefore, H_0 and L_0 of seal rings should be small enough on the premise that leakage does not occur.

4.2 Case study: process optimization based on optimal contact pressure path

Effects of P_v on axial displacement of the ring-shaped blank are investigated by taking the forming of thin-walled corrugated rings as an example (see Fig. 9). Two types of corrugated rings (type A and type B) are studied in this work, both of which are of large diameter-thickness ratio ($D_0/t_0 = 767$), i.e., parts with larger outer diameter and extremely thin wall (0.3 mm). Meanwhile, the diameter variation along axial direction is relatively large (diameter variation of 7.2 mm in 1.4-mm axial length). The low rigidity and regional complex geometry of these parts increase the difficulty of manufacture.

The forming strategy of "type A" parts is illustrated in Fig. 10a. Apparently, the structure of die cavity determines how difficult metal blank enters into the die cavity, thus has strong correlation with P_v. The structure of die cavity is considered to be determined by the surface radius of the entrance of die cavity (R) and the width of the die cavity (L). FEA was conducted to find the optimized value of R and L. The load path 9 of contact pressure shown in Fig. 6b is taken as a reference for the optimization of P_v. If P_v varies in accordance

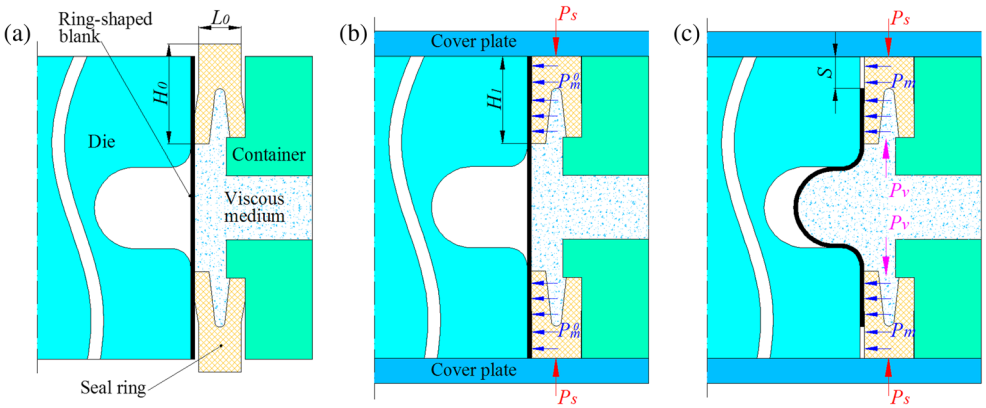

Fig. 8 Sealing of viscous medium. **a** Initial stage. **b** Die closing stage. **c** Forming stage

Table 4 Axial displacement (S) corresponding to seal rings with different sizes

Type	1	2	3	4	5	6	7	8	9
H_0 (mm)	14.0	14.0	14.0	13.5	13.5	13.5	13.0	13.0	13.0
L_0 (mm)	6.0	5.5	5.0	6.0	5.5	5.0	6.0	5.5	5.0
S (mm)	0.92	0.97	1.01	0.96	1.00	1.04	0.98	1.02	1.05

with load path 9, the total contact pressure subjected by the ring-shaped blank varies in a similar way. The structure of die cavity and the process design in this condition were recognized as reasonable. Here, the static pressure (P_s) is supposed to be constant for all cases.

The ring-shaped blank was preformed through diameter expanding process at first to get a preformed shape (see Fig. 11a). The diameter expanding process was not taken into consideration because of the ignorable amount of deformation. The resultant relationship between cavity pressure (i.e., pressure of viscous medium) and piston stoke is given in Fig. 10b. When R = 3 mm and L = 1 mm, the cavity pressure increases sharply and reaches a maximum value of about 200 MPa within the piston stroke of 1 mm. Then, excessive thinning or fracture will be inevitable. It is attributed to the narrow entrance of die cavity, which inhibits the filling of metal blank. In general, the path of cavity pressure (P_v) gradually approaches to the ideal one (load path 9) with the increase of R and L. However, when R and L exceed 5 and 3 mm, the variation tends to be smaller.

Based on these results, the die cavity was designed with R of 10 mm and L of 3 mm. In this condition, the cavity pressure varies closely to the ideal pressure path (see Fig. 10b). S in two extreme cases is compared (see Fig. 11a, b). A 33% increase (0.6 mm) of S is observed in the case that die structure is optimized. In the optimal condition, the experimental value of axial displacement for SUS321 and GH4169 parts are separately 2.6 and 2.53 mm, which are close to the theoretical value of 2.7 mm (see Fig. 11c). The reason lies in the fact that the axial displacement of the ring-shaped blank can keep up with the filling of viscous medium and metal blank towards the die cavity in the optimal condition. The wide entrance of die cavity is beneficial to lower down the resistance.

4.3 Forming experiments

The optimal die structure presented in Fig. 11b was adopted in the forming experiments of thin-walled corrugated rings (type A). The welded ring-shaped metal blank was employed as initial blank. A two-step forming process was designed for "type A" part as shown in Fig. 12a, b. The ring-shaped blank was firstly expanded slightly to get the preformed shape through diameter expanding process. Then, diameter reducing process was carried out to obtain the final shape of "type A" part. In order to manufacture "type B" part, additional diameter expanding procedure was implemented as shown in Fig. 12c. Seal rings were positioned on both ends of the ring-shaped blank.

Experimental part is shown in Fig. 13. Experimental parts were cut along diameter direction by electric discharge machining (EDM). The longitudinal section and wall thickness distribution are given in Fig. 14. The maximum thickness thinning of SUS321 and GH4169 parts are separately 7 and 8%, which is considered to be small enough to meet with the usage requirements. Thickness distribution obtained from experiments and FEA agree well. The axial displacement of the ring-shaped blank can be used to explain the smaller thickness thinning. In addition, GH4169 parts show more wall thickness thinning than SUS321 parts. Since the yield strength of GH4169 sheet is larger than SUS321 sheet, the GH4169 parts are subjected to larger tensile stress along meridian direction than SUS321 parts.

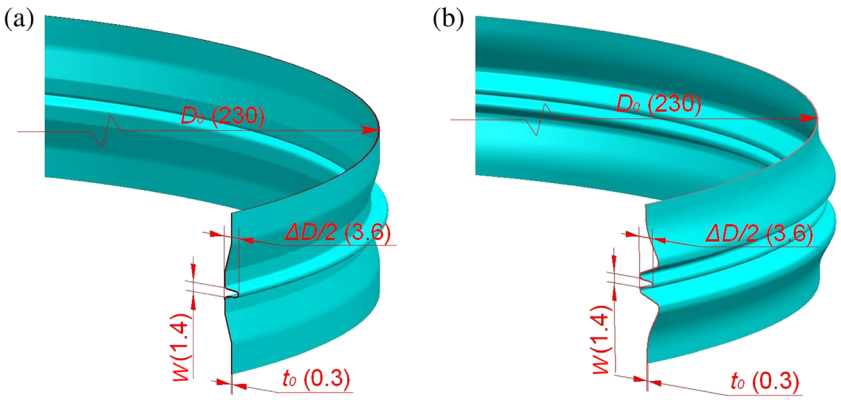

Fig. 9 Thin-walled corrugated rings. **a** Type A. **b** Type B (unit mm)

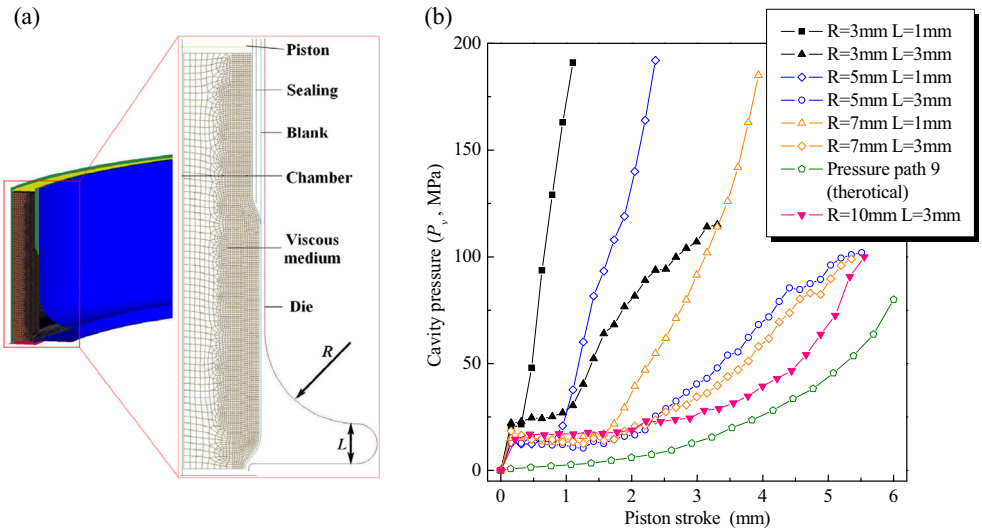

Fig. 10 Cavity pressure corresponding to different die structure. **a** Finite element model. **b** Cavity pressure versus punch stroke

Because of the similar geometrical characteristic between "type B" and "type A" parts, "type B" parts can be formed through performing an additional diameter expanding process on the basis of "type A" parts (see Fig. 12c). By employing the same design strategy, the die structure used for the manufacture of "type B" parts was worked out. Experimental part and thickness distribution of "type B" part are shown in Fig. 15. The maximum thickness thinning of SUS321 and GH4169 parts are respectively 8.7 and 9%. The slight increase of thickness thinning comparing with "type A" parts is related to the repeated pressure subjected by "type B" parts. The axial displacement of blank ends for SUS321 and GH4169 parts are respectively 4.63 and 4.46 mm (the theoretical value is 5.1 mm). Also, the thickness thinning is acceptable and the blank draw-in is possible to inhibit the stretching of blank material.

4.4 Evaluation of the forming strategy

The key factor to facilitate metal flow in proposed forming strategy is the utilization of viscous medium. Differing from conventional fluid medium such as oil, viscous medium is of high viscosity. Rosel and Merklein once employed oil and MR fluid as forming medium in

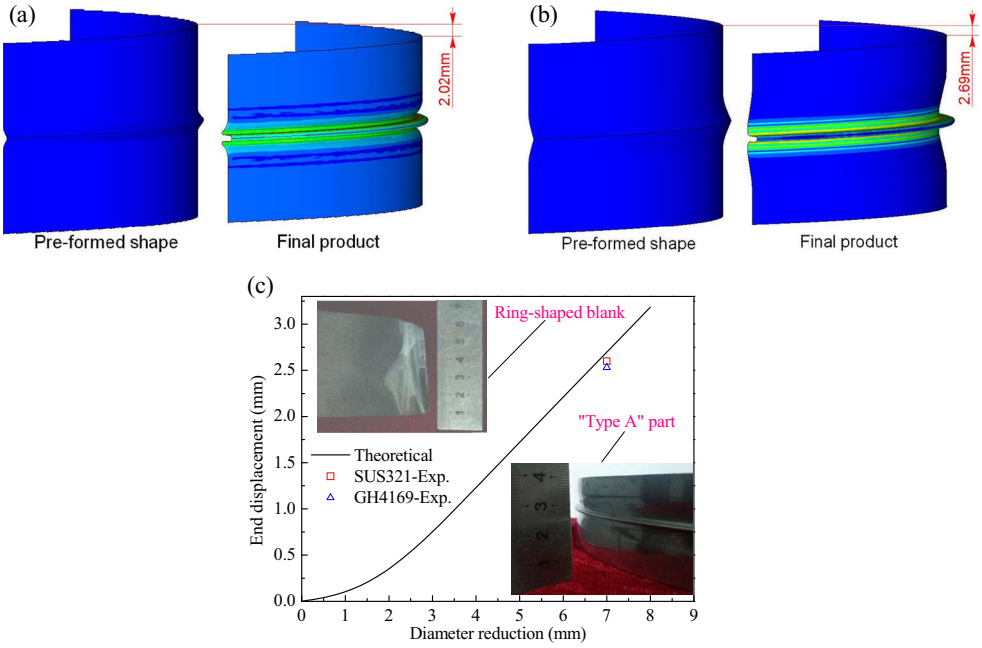

Fig. 11 End displacement in experiment and FEA corresponding to different die structure. **a** S in the simulated case of $R = 3$ mm and $L = 1$ mm. **b** S in the simulated case of $R = 10$ mm and $L = 3$ mm. **c** S in the experimental case of $R = 10$ mm and $L = 3$ mm

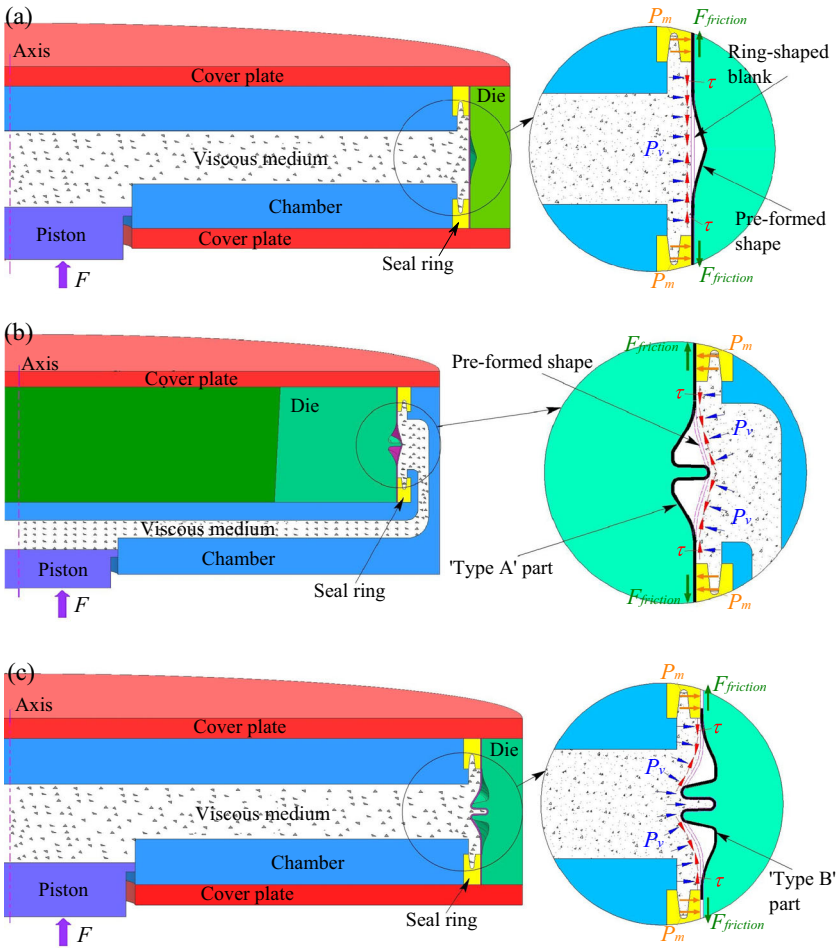

Fig. 12 Forming procedures. **a** Pre-forming process. **b** Diameter reducing process. **c** Diameter expanding process

sheet hydroforming process [19]. They stated that MR fluid will achieve the same cavity pressure at a lower flange contact pressure compared with mineral oil. It is attributed to the higher viscosity of MR fluid under magnetic field. Then, sheet metal blank flows into the cavity easily and thickness thinning is reduced. According to Eq. 1, the sealing limit of MR fluid is lower than that of mineral oil. That is to say, the smaller sealing limit leads to enhanced metal flow.

The shear viscosity of silicon oil, MR fluid (serving under magnetic field of 0.13 T), and viscous medium is measured in this work as shown in Table 5. The viscosity of viscous medium is 170,000 times larger than that of silicon oil and 357 times larger than that of MR fluid. Then, the contact pressure

Fig. 13 Thin-walled corrugated ring (type A)

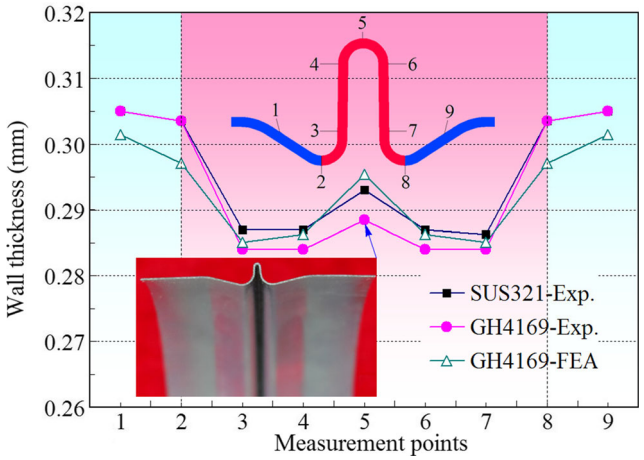

Fig. 14 Wall thickness distribution of experimental specimen (type A)

at seal ring/blank interface in the quasi-bulk forming is definitely lower than that in hydroforming employing oil as forming medium for the same cavity pressure. Therefore, sealing limit of viscous medium is much smaller than that of mineral oil. In addition, in the case that mineral oil is employed, the sealing structure shown in Fig. 8 is no longer applicable since the contact pressure of this structure is too small to avoid leakage.

Then, the mechanism of the forming strategy can be interpreted as follows. On the one hand, the optimal die structure facilitates the filling of viscous medium and metal blank towards the die cavity, which may lower down the cavity pressure (P_v). The seal rings are then compressed less. Accordingly, contact pressure (P_m) at blank ends decreases and the material of ring-shaped blank is less stretched. On

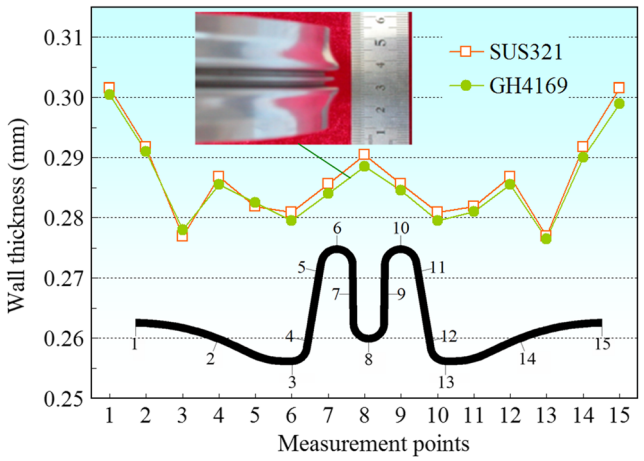

Fig. 15 Wall thickness distribution of thin-walled corrugated ring with meridian (type B)

Table 5 Shear viscosity of silicon oil, MRF, and viscous medium

Description	Unit	Silicon oil	MRF	Viscous medium
Shear viscosity at 25 °C	Pa·S	0.1	47.5	17,000

the other hand, the highly viscous medium brings down the sealing pressure. Blank ends will not be constrained tightly. Thus, the constraining force at blank ends decreases, which also facilitates the metal flow. The forming range is extended. Therefore, the application of this forming strategy for other types of thin-walled corrugated parts with complex shapes will be expectable as well.

5 Conclusions

Based on the previous study on quasi-bulk forming process, forming strategy of thin-walled corrugated rings was further investigated in this paper. The sealing mechanism and process optimization based on the load path of contact pressure at blank ends were discussed. The following conclusions can be drawn from FEA and experimental results:

1. Compared with conventional mineral oil, sealing limit of the highly viscous medium tends to be smaller. That results in a smaller constraining force subjected by blank ends. The available range of contact pressure without leakage is thus extended.
2. In the condition that viscous medium serves as flexible die and appropriate sealing strategy is adopted, contact pressure (P_m) at seal ring/blank interface can be adjusted. It will be beneficial to inhibit thickness thinning of corrugated rings with extremely thin wall.
3. Seal rings are compressed by the combined action of static pressure (P_s) and cavity pressure (P_v), both of which constitute the contact pressure (P_m) at seal ring/blank interface. The optimal load path of P_m is presented and taken as a reference for process optimization. The reasonable die structure is designed to keep the path of P_v approximate to the optimal load path of contact pressure. By this way, metal flow is improved.
4. Based on aforementioned forming strategy, two types of SUS321 and GH4169 parts were successfully produced. The thickness thinning is relatively smaller and the axial displacement of the ring-shaped blank is considered to be sufficient. The validity of the design strategy is verified.

Acknowledgements The presented investigations have been supported by the National Natural Science Foundation of China (No. 51275130) and Program for Changjiang Scholars and Innovative Research Team in University (No.IRT1229). The authors kindly acknowledge these supports.

References

1. Elyasi M, Bakhshi-Jooybari M, Gorji AH (2010) A new die design for the hydroforming of stepped tubes. Int J Mater Form 3:71–75
2. Chan LC, Ricky Kot WK (2014) Determination of loading paths in warm hydroforming reinforced quadrilateral tubular components. Mater Manuf Process 29:32–36
3. Wang G, Zhang KF, Wu DZ, Wang JZ, Yu YD (2006) Superplastic forming of bellows expansion joints made of titanium alloys. J Mater Process Technol 178:24–28
4. Ganesh P, Senthil Kumar VS (2014) Superplastic forming of friction stir welded AA6061-T6 alloy sheet with various tool rotation speed. Mater Manuf Process 30:1080–1089
5. Maeno T, Mori K, Adachi K (2014) Gas forming of ultra-high strength steel hollow part using air filled into sealed tube and resistance heating. J Mater Process Technol 214:97–105
6. Liu G, Wu Y, Wang DJ, Yuan SJ (2015) Effect of feeding length on deforming behavior of Ti-3Al-2.5 V tubular components prepared by tube gas forming at elevated temperature. Int J Adv Manuf Technol 81:1–8
7. Ohashi T, Hayashi K (2003) Lateral extrusion of A6063 aluminum alloy pipes with a lost core. J Mater Process Technol 138:560–563
8. Ohashi T, Matsui K, Saotome Y (2001) The lateral extrusion of copper pipes with a lost core of low temperature melting alloy. J Mater Process Technol 113:98–102
9. Furushima T, Hung NQ, Manabe KI, Sasaki O (2013) Development of semi-dieless metal bellows forming process. J Mater Process Technol 213:1406–1411
10. Wei SG, Xu LP, He K, Li JH, Wei F, Du R (2015) Experimental study on manufacturing metal bellows forming by water jet incremental forming. Int J Adv Manuf Technol 81:129–133
11. Lorenzo RD, Ingarao G, Chinesta F (2009) A gradient-based decomposition approach to optimize pressure path and counterpunch action in Y-shaped tube hydroforming operations. Int J Adv Manuf Technol 44:49–60
12. Louh MM, Meysam S (2008) Numerical study on effect of bilinear pressure path on corner filling in hydroforming of tube in box-shape die. J Solid Mech in Eng 1:77–86
13. Faraji G, Mashhadi MM, Norouzifard V (2009) Evaluation of effective parameters in metal bellows forming process. J Mater Process Technol 209:3431–3437
14. Kang BH, Lee MY, Shon SM (2007) Forming various shapes of tubular bellows using a single-step hydroforming process. J Mater Process Technol 194:1–6
15. Bakhshi-Jooybari M, Elyasi M, Gorji A (2010) Numerical and experimental investigation of the effect of the pressure path on forming metallic bellows. Proc Inst Mech Eng, Part B 224:95–101
16. Wang ZJ, Xiang N, Yi J, Song H (2016) Forming thin-walled circular rings with corrugated meridians via quasi-bulk deformation of metal blank and viscous medium. J Mater Process Technol 236:35–47
17. Xiang N, Wang ZJ, Yi J, Song H (2016) Extending the forming of thin-walled metal circular rings with corrugated meridians to a process without axial compression. Int J Adv Manuf Technol 86:651–661
18. Hein P (1999) Innenhochdruck-Umformen von Blechpaaren: Modellierung, Prozessauslegung und Prozessführung. In: Geiger M, Feldmann, K (Hrsg) Reihe Fertigungstechnik, Band 96, Bamberg, Meisenbach.
19. Rösel S, Merklein M (2014) Improving formability due to an enhancement of sealing limits caused by using a smart fluid as active fluid medium for hydroforming. Prod Eng Res Devel 8:7–15
20. Wang ZJ, Liu JG, Wang XY (2004) Viscous pressure forming (VPF): state-of-the-art and future trends. J Mater Process Technol 151:80–87
21. Groche P, Ertuğrul M (2008) Process control at the sealing line during sheet metal hydroforming. Prod Eng Res Devel 2:3–8
22. Qin CH, Zhang XC, Ye S, Tu ST (2015) Grain size effect on multi-scale fatigue crack growth mechanism of nickel-based alloy GH4169. Eng Fract Mech 142:140–153
23. Yadav US, Yadava V (2014) Parametric study on electrical discharge drilling of aerospace nickel alloy. Mater Manuf Process 29:260–266
24. Adam Khan M, Sundarrajan S, Natarajan S, Parameswaran P, Mohandas E (2014) Oxidation and hot corrosion behavior of nickel-based superalloy for gas turbine applications. Mater Manuf Process 29:832–839
25. Liu J, Westhoff B, Ahmetoglu M, Altan T (1996) Application of viscous pressure forming (VPF) to low volume stamping of difficult-to-form alloys—results of preliminary FEM simulations. J Mater Process Technol 59:49–58
26. Gao TJ, Wang ZJ, Deng JD (2007) Influence of necking length on viscous medium outer pressure necking forming. Forg Stamping Technol 32:23–25 (in Chinese)
27. Ahmetoglu M, Jiang H, Kulukuru S, Altan T (2004) Hydroforming of sheet metal using a viscous pressure medium. J Mater Process Technol 146:97–107